# Asymmetry of fibrillar plaque burden in amyloid mouse models

**Christian Sacher[1], Tanja Blume[1,2], Leonie Beyer[1], Gloria Biechele[1], Julia Sauerbeck[1], Florian Eckenweber[1], Maximilian Deussing[1], Carola Focke[1], Samira Parhizkar[3], Simon Lindner[1], Franz-Josef Gildehaus[1], Barbara von Ungern-Sternberg[1], Karlheinz Baumann[4], Sabina Tahirovic[2], Gernot Kleinberger[3,5,6], Michael Willem[3], Christian Haass[2,3,5], Peter Bartenstein[1], Paul Cumming[7,8], Axel Rominger[1,7], Jochen Herms[2,5,9], Matthias Brendel[1,5]**

[1]Dept. of Nuclear Medicine, University Hospital of Munich, LMU Munich, Munich Germany

[2]DZNE - German Center for Neurodegenerative Diseases, Munich, Germany

[3]Chair of Metabolic Biochemistry, Biomedical Center (BMC), Faculty of Medicine, LMU Munich, Munich, Germany

[4]Roche Pharma Research and Early Development, F. Hoffmann-La Roche Ltd., Basel, Switzerland

[5]Munich Cluster for Systems Neurology (SyNergy), Munich, Germany

[6]ISAR Bioscience GmbH, Planegg, Germany

[7]Department of Nuclear Medicine, Inselspital, University Hospital Bern, Bern, Switzerland

[8]School of Psychology and Counselling and IHBI, Queensland University of Technology, Brisbane, Australia

[9]Center of Neuropathology and Prion Research, University of Munich, Munich Germany

**Abbreviated title:** Aβ plaque asymmetry in mice

**Corresponding author:** Dr. Matthias Brendel; Department of Nuclear Medicine, University of Munich; Marchioninistraße 15, 81377 Munich, Germany; Phone:+49(0)89440074650, Fax:+49(0)89440077646; E-Mail:matthias.brendel@med.uni-muenchen.de

**First author:**
Christian Sacher (medical student); Department of Nuclear Medicine; LMU Munich, Germany; Phone:+49(0)1623878661; E-Mail:christian.sacher@med.uni-muenchen.de

**Word count:** 5000

## ABSTRACT

**Objective:** Asymmetries of amyloid-β (Aβ) burden, are well-known in Alzheimer's disease (AD), but did not receive attention in Aβ mouse models of AD. Therefore, we investigated Aβ-asymmetries in Aβ mouse models examined by Aβ- small animal positron-emission-tomography (PET) and tested if such asymmetries have an association with microglial activation. **Methods:** 523 cross-sectional Aβ-PET scans of five different Aβ mouse models (APP/PS1, PS2APP, APP-SL70, $App^{NL\text{-}G\text{-}F}$ and APPswe) were analyzed together with 136 18kDa translocator protein (TSPO)-PET scans for microglial activation. The asymmetry index (AI) was calculated between tracer uptake in both hemispheres. AIs of Aβ-PET were analyzed in correlation with TSPO-PET AIs. Extrapolated required sample sizes were compared between analyses of single and combined hemispheres. **Results:** Relevant asymmetries of Aβ deposition were identified in ≥30% of all investigated mice. There was a significant correlation between AIs of Aβ-PET and TSPO-PET in four investigated Aβ mouse models (APP/PS1: $R$=0.593, $P$=0.001; PS2APP: $R$=0.485, $P$=0.019; APP-SL70: $R$=0.410, $P$=0.037; $App^{NL\text{-}G\text{-}F}$: $R$=0.385, $P$=0.002). Asymmetry was associated with higher variance of tracer uptake in single hemispheres, leading to higher required sample sizes. **Conclusions:** Asymmetry of fibrillar plaque neuropathology occurs frequently in Aβ mouse models and acts as a potential confounder in experimental designs. Concomitant asymmetry of microglial activation indicates a neuroinflammatory component to hemispheric predominance of fibrillary amyloidosis.



**Key words:** asymmetry, amyloid, microglia, mouse models

## INTRODUCTION

Alzheimer disease (AD) is the most frequent neurodegenerative disease, with burgeoning incidence rates due to the rising life expectancy in most of the world (*1*). The neuropathology of AD is histologically characterized by the triad of accumulation of amyloid-β peptide (Aβ) as extracellular plaques, fibrillary tau aggregates within neurons, and the activation of multiple neuroinflammatory pathways, which is mediated by activated microglia expressing high levels of the marker 18-kDa translocator protein (TSPO) (*2*). Animal models that accurately reflect this complex pathology are indispensable for contemporary preclinical research into the molecular mechanisms of AD. In this context, a range of different overexpressing and knock-in Aβ mouse models have been established for molecular imaging with positron emission tomography (PET). In recent PET studies, increased binding of the Aβ tracer $^{18}$F-florbetaben ($^{18}$F-FBB) and the TSPO tracer $^{18}$F-GE-180 were firmly established by longitudinal *in vivo* quantification of cerebral amyloidosis and microglial activation in various Aβ mouse models of AD (*3-5*). In humans, an asymmetric spatial distribution of neuropathological AD hallmarks is frequently discovered by PET studies *in vivo* *(6-8)*. A recent human PET study has already shown that asymmetric spatial distributions of Aβ plaques are positively correlated with ipsilateral neurodegeneration (*8*). However, no study has hitherto investigated systematically the asymmetry in Aβ mouse models of AD. While a large scaled investigation of this phenomenon by histopathological investigations would be of high economic effort and difficult in terms of standardization, *in vivo* PET imaging methods should afford the means to compare readily the Aβ plaque burden in both hemispheres of individual animals.

Given this background, our aim was to investigate the occurrence of asymmetric fibrillar Aβ deposition in the well-established Aβ mouse models APP/PS1, PS2APP, APP-SL70, *App*$^{NL-G-F}$ and APPswe. Using a large series of historical $^{18}$F-FBB Aβ-PET recordings, we tested for asymmetric Aβ deposition, while

considering age as a predictive variable. We also made sample size estimations for detecting asymmetric Aβ, and tested the hypothesis that Aβ asymmetry is associated with ipsilateral microglial activation as assessed by $^{18}$F-GE-180 TSPO-PET.

## MARTERIAL AND METHODS

### Experimental Design

All experiments were performed in compliance with the National Guidelines for Animal Protection, Germany and with the approval of the regional animal committee (Regierung Oberbayern) and were overseen by a veterinarian. Animals were housed in a temperature- and humidity-controlled environment with 12h light-dark cycle, with free access to food (Sniff, Soest, Germany) and water. A detailed overview of the investigated mouse cohorts is given in Supplemental Table 1. All PET raw data originated from previous in-house studies (cited below) conducted on the same Inveon small animal PET under identical acquisition parameters. 87% of the mice investigated were female. APP/PS1 and APPswe comprised only female mice, whereas PS2APP, APP-SL70, and *App*$^{NL-G-F}$ included both sexes. All raw data were reprocessed to guarantee optimal agreement of spatial and radioactivity normalization. Either descriptive datasets or control groups of therapy/ genotype studies were included. From each investigated mouse, the degree of asymmetry in Aβ-PET and TSPO-PET was assessed by volume-of-interest based quantification in both cerebral hemispheres.

### Animal Models

*APP/PS1 (APPPS1-21):* This transgenic mouse model was generated on a C57BL/ 6J genetic background that coexpresses KM670/671NL mutated amyloid precursor protein and L166P mutated presenilin 1 under the control of a neuron-specific Thy1 promoter. Cerebral amyloidosis in this model starts at 6–8 weeks of age (*9*). Historical $^{18}$F-FBB data from 41 scans of APP/PS1 mice imaged at four

different ages (3, 6, 9 and 12 months) were reprocessed (*10*). 27 contemporaneous $^{18}$F-GE-180 scans were available.

*PS2APP (APPswe/PS2):* The transgenic B6.PS2APP (line B6.152H) is homozygous both for human presenilin (PS) 2, the N141I mutation, and the human amyloid precursor protein (APP) K670N/M671L mutation (*11*). Homozygous B6.PS2APP mice show first appearance of plaques in the cerebral cortex and hippocampus at 5–6 months of age (*12*). Historical $^{18}$F-FBB data from 147 scans of PS2APP mice imaged at four different age ranges (6–8, 9–10, 11–14 and 15–17 months) were reprocessed (*13,14*). 23 contemporaneous $^{18}$F-GE-180 scans from these mice were likewise reprocessed by standard methods.

*APP-SL70:* The PS1 knock-in line was generated by introducing two-point mutations in the wild-type mouse PSEN1, corresponding to the mutations M233T and L235P. The APP751SL mouse overexpresses human APP751 carrying the London (V717I) and Swedish (K670N/M671L) mutations under the control of the Thy1 promoter. Aβ deposits appear as early as 2.5 months of age in these mice (*15*). Historical $^{18}$F-FBB data from 208 scans of APP-SL70 mice imaged at four different ages (4–6, 7–9, 10–12 and 13–15 months), deriving from a descriptive observational study (*16*), along with control scans from an as yet unpublished therapy study were reprocessed. 26 contemporaneous $^{18}$F-GE-180 scans were available in this group.

*App$^{NL-G-F}$ (App$^{NL-G-F/NL-G-F}$)*: The knock-in mouse model *App$^{NL-G-F}$* carries a mutant APP gene encoding the humanized Aβ sequence (G601R, F606Y, and R609H) with three pathogenic mutations, namely Swedish (KM595/596NL), Beyreuther/Iberian (I641F), and Arctic (E618G). Homozygotic *App$^{NL-G-F}$* mice progressively exhibit widespread Aβ accumulation from two months of age (*17,18*). Historical $^{18}$F-FBB data from 55 scans of homozygotic *App$^{NL-G-F}$* mice imaged at four different ages (2.5, 5.0, 7.5 and 10 months) were reprocessed (*3*). 55 contemporaneous $^{18}$F-GE-180 scans were available in this data set.

*APPswe:* Transgenic mice overexpressing human APP with the Swedish double

mutation (K670N, M671L) driven by the mouse Thy1.2 promoter were generated as described earlier (*11*). Mice heterozygous for the transgene begin accumulating β-amyloid at approximately nine months of age and develop β-amyloid plaques at twelve months of age, mainly in the cortical mantle. Historical $^{18}$F-FBB data from 72 scans of APPswe mice imaged at three different age ranges (9–12, 13–16 and 17–20 months) were reanalyzed (*19,20*). Contemporaneous $^{18}$F-GE-180 scans were not available for these mice.

*C57Bl/6:* Historical and unpublished $^{18}$F-FBB data from 27 scans of C57Bl/6 mice (WT) were reprocessed and served as control material (age: 2.5-16 months).

**PET Imaging**

*PET Data Acquisition, Reconstruction and Post-Processing:* For all PET procedures, radiochemistry, data acquisition, and image pre-processing were conducted according to an established, standardized protocol (*4,21*). In brief, $^{18}$F-FBB Aβ PET recordings (average dose: 11.4±2.0 MBq) with an emission window of 30–60 min after injection were obtained to measure fibrillar cerebral amyloidosis. $^{18}$F-GE-180 TSPO PET recordings (average dose: 11.1±2.0 MBq) with an emission window of 60–90 min after injection were performed for assessment of cerebral TSPO expression. Anesthesia was maintained from just before tracer injection to the end of the imaging time window.

*PET Image Analysis:* We performed all analyses using PMOD (version 3.5; PMOD technologies). Normalization of emission images to standardized uptake value ratio (SUVR) images was performed using previously validated white matter (WM) reference regions for transgenic amyloid mouse models (APP/PS1, PS2APP, APP-SL70 and APPswe) (*4,21*). For the knock-in mouse line *App*$^{NL-G-F}$, the mesencephalic periaqueductal gray (PAG) was used as reference region, as recently published (*3*). Two bilateral telencephalic volumes of interest (VOIs) (containing cortex and hippocampus) comprising 50 mm$^3$ each, were employed for calculation of

$SUVR_{Forebrain/WM}$ or $SUVR_{Forebrain/PAG}$. For each scan, the hemispheric asymmetry index (AI) was calculated for $^{18}$F-FBB or $^{18}$F-GE-180 scans using the formula:

$$AI\ [\%] = 200 \times (R - L) / (R + L)$$

.

**Statistical Analysis**

95% and 99% confidence intervals (CI) of $^{18}$F-FBB AIs in normal C57BL/6 mice were calculated. Aβ mouse model $^{18}$F-FBB scans were judged as asymmetric when they exceeded the 95%-CI (moderate asymmetry) or the 99%-CI (strong asymmetry) of C57BL/6 mice. Significant $^{18}$F-FBB |AIs| (absolute magnitude) were correlated with age for each Aβ mouse model to evaluate age-dependency of asymmetric plaque distribution. For each Aβ mouse model, age-independent lateralized plaque distributions were compared by a Chi-square test to test for left or right predominance of Aβ deposition. Frequency of strong asymmetries were calculated in groups of comparable age for Aβ mouse models and correlated with coefficients of variance (CoV) of SUVR in the same groups of mice. Pearson's coefficients of correlation (*R*) were calculated for the latter analyses and for correlation analyses between $^{18}$F-FBB AIs and age as well as between $^{18}$F-FBB AIs and $^{18}$F-GE-180 AIs. Hypothetical 2-sided t-test of independent measures were performed in order to perform sample sizes calculations in comparison of SUVR in single hemispheres and in combined hemispheres using G*Power (V3.1.9.2, Kiel, Germany). We used a given 5% therapy effect on SUVR at a power (1–β) of 0.80 and type one error of α=0.05. A *P*-value of less than 0.05 was considered to be significant for rejection of the null hypothesis. SPSS 25 statistics (IBM Deutschland GmbH, Ehningen, Germany) was used for all statistical tests.

**RESULTS**

**Asymmetric Plaque Distribution is Frequent in Aβ Mouse Models**

First, we defined an asymmetry threshold based on PET measurements in

WT mice to establish real Aβ asymmetry, without bias in the spatial normalization or by physiological variability in tracer uptake. The 95%-CI of $^{18}$F-FBB AIs in C57BL/6 mice was -3.6% (right lateralization) to 3.6% (left lateralization) and defined the threshold for moderate Aβ asymmetry. The 99%-CI of $^{18}$F-FBB AIs in C57BL/6 was -4.0% (right lateralization) to 4.5% (left lateralization) and defined the threshold for strong Aβ asymmetry. Using these thresholds, 40% (L=21%; R=19%; 95%-CI) of all amyloid accumulating mice showed moderate asymmetry and 30% (L=14%; R=16%; 99%-CI) showed strong asymmetry of $^{18}$F-FBB forebrain uptake (Figure 1). There was no significant hemispheric predominance across the whole cohort of different Aβ mouse models. A detailed overview is provided in Supplemental Table 1.

Highest frequency of moderate Aβ-PET asymmetry was observed in PS2APP and *App*$^{NL-G-F}$ mice (49% each). Strong Aβ-PET asymmetry was most frequently observed in PS2APP and APP/PS1 mice (37% each). Lowest frequency of Aβ-PET asymmetry was present in APPswe mice, in which 32% of scans indicated moderate and 24% showed strong asymmetry. A significant left-hemispheric predominance of Aβ deposition was detected in the PS2APP mice ($\chi^2$=4.7; *P*=0.030; Chi-square test), whereas a significant right-hemispheric predominance of Aβ deposition was seen in APPswe mice ($\chi^2$=15; *P*=0.0001; Chi-square test). There was no significant association between age and asymmetric Aβ distribution in any Aβ mouse model (Figure 2). In summary, asymmetry of plaque burden was frequently observed in all studied Aβ mouse models, but with different magnitudes and side predilections.

**Asymmetric Plaque Burden Impacts the Sufficient Sample Sizes in Preclinical Trials**

Given the observed asymmetries in all Aβ mouse models studied, we hypothesized that measures in single hemispheres (as are typically examined by histological methods) would suffer from higher variance, subsequently leading to higher required sample sizes in preclinical trials when compared to combined

measures of both hemispheres, as are obtained by PET. CoV were positively associated with the frequency of plaque burden asymmetry (99%-CI) in groups of comparable age in different Aβ mouse models ($R$=0.380, $P$=0.027, Figure 3A). CoV by groups of comparable age in the different Aβ mouse models were 4.3±1.2% for separate measures of left and right hemispheres and significantly lower for the combined quantification of both hemispheres (3.9±1.2%; $P$ = left vs. both: 0.0003/ right vs. both: 0.0007; paired $t$-test). Calculated sample sizes for detection of a 5% therapy effect on SUVR at a power (1–β) of 0.80 and type one error of α=0.05 were n=14.1 for separate measures for the left hemisphere, n=13.9 for separate measures of the right hemisphere, and n=11.9 for combined quantification of both hemispheres ($P$=0.0020/0.0016; paired $t$-test). Required sample sizes as a function of power were consistently higher for calculation with left (Figure 3B) and right (Figure 3C) hemispheric values when compared to combined quantification of both hemispheres. The average reductions of required sample sizes for combined quantification of both hemispheres were 2.1±0.6 (vs. left) and 1.8±0.5 (vs. right). These results indicate that asymmetry of plaque burden in Aβ mouse models considerably increases required sample sizes when hemispheres are analyzed separately.

**Asymmetric Plaque Burden is Associated with Ipsilateral Glial Activation**

Several studies have revealed associations between amyloid deposition and microglial activation in Aβ mouse models (*3,4,16*). However, it has not hitherto been investigated if microglial activation follows any asymmetry of plaque burden, or if the microgliosis is globally distributed. Hence, we made use of contemporaneous TSPO-PET data for correlation analysis with lateralization to Aβ-PET. Significant positive associations between asymmetric Aβ deposition and ipsilateral lateralization of TSPO expression were observed in all four Aβ mouse models. The magnitude of correlation between asymmetric Aβ-PET and ipsilateralized TSPO-PET uptake was similar among APP/PS1 ($R$=0.593; $P$=0.001; n=27; Pearson's correlation), PS2APP

(*R*=0.485; *P*=0.019; n=23; Pearson's correlation), APP-SL70 (*R*=0.410; *P*=0.037; n=26; Pearson's correlation), and *App*$^{NL-G-F}$ (*R*=0.385; *P*=0.002; n=60; Pearson's correlation) mice. Taken together these results clearly indicate a spatial association between asymmetric distribution of fibrillar Aβ plaques and ipsilateral microglial activation.

## DISCUSSION

In contrast to human investigations on asymmetrical Aβ distribution in AD (*6,8,22*), only scantly evidence is available for the presence of Aβ asymmetry in mouse models (*19,23*). We present the first large-scale preclinical *in vivo* investigation of fibrillar plaque burden asymmetry by standardized evaluation of PET data. With respect to animal welfare guidelines, in particular reduction of animal numbers in accordance with the 3R principle, we used scans from various earlier studies, this avoiding any requirement for additional animal experiments to test our hypotheses.

First, we endeavored to establish a reasonable threshold of lateralized Aβ-PET signal to exclude asymmetry findings driven by reasons other than Aβ pathology. To this end, we used Aβ-PET data of C57BL/6 WT mice, as they are not known to manifest any Aβ accumulation. Minor asymmetry of FBB tracer uptake in WT mice could be attributed to factors such as differences in cerebral blood flow, differing hemispheric volumes, or methodological issues such as lateralized spill-over of bone uptake, imperfect attenuation correction, or bias in spatial normalization. Hence, we used the 95% and 99% CIs of $^{18}$F-FBB AIs in WT to discern moderate and strong asymmetry in the groups of Aβ accumulating mice. By these criteria, 40% of all Aβ accumulating mice revealed moderate asymmetry, and 30% showed strongly asymmetric Aβ deposition, but without evidence for a general lateralization across all AD models. Nevertheless, two out of five investigated amyloid models

revealed significant lateralization of Aβ plaque distribution to Aβ-PET. There was a significant left-hemispheric predominance of Aβ deposition in PS2APP mice, but a significant right-hemispheric predominance in APPswe mice. While molecular explanations and causal mechanisms giving rise to this phenomenon are presently unknown, we contend that this is a real phenomenon requiring special consideration when comparing data from different Aβ mouse models of AD. For example, a comparison of exclusively right hemisphere read-outs, as might be obtained by histological analysis, between APPswe and PS2APP could cause false negative findings, and likewise for the left hemisphere. The highest frequency of asymmetry was observed in Aβ models with a Presenilin mutation (PS2APP and APP/PS1), indicating that involvement of this gene might increase the probability of asymmetric plaque burden. Variable expression of APP mRNA across different PS2APP mice is already postulated to be a key determinant of variance in individual Aβ deposition (*12*); therefore we speculate that this phenomenon could likewise hold true for differences between hemispheres.

By making sample size estimations, we established that the observed asymmetries of fibrillar plaque burden are potentially relevant to the design of preclinical trials. Importantly, the calculated sample sizes sufficient to detect relevant therapeutic effects, which are comparable to those of earlier drug trials in these Aβ mouse models (*13,20*), were significantly higher when only single hemispheres were analyzed, as opposed to combined measurement of both hemispheres. As Aβ-PET and histology markers for fibrillar Aβ were strongly intercorrelated in previous studies (*10,19,24*), we assume that asymmetry effects on required sample sizes should also hold true for stand-alone histological or biochemical analyses. This conjecture remains to be demonstrated, since usual practice is to process one hemisphere for histology and one for biochemistry. Aβ-PET findings at the terminal time-point could help to identify mice with asymmetric plaque burden, which would allow consecutive adjustment of measures by different modalities in separate hemispheres.

Next, we investigated whether asymmetric Aβ distributions occur in an age-dependent manner. Our cross-sectional analysis of historical PET data did not indicate any significant association of AI with age among the five Aβ mouse models. This is consistent with our earlier longitudinal $^{18}$F-FBB-PET findings in APPswe, were we incidentally noticed that some animals showed consistently right-sided plaque asymmetry between 13 and 20 months of age. More precisely, the magnitude of asymmetry in SUVR increased with age, but with no temporal dependence of the AI *per se* (*19*). In conclusion, Aβ asymmetries, when present, are established at the onset of plaque deposition.

We suppose that there are hitherto few reports on asymmetric plaque burden in Aβ mouse models due to the logistic difficulty of conducting onerous histological analysis of both hemispheres for sufficient numbers of animals. We performed a meta-analysis of the most recent 56 papers from journals with impact factor > 4 published in the interval 2016 to 2019 with the key words “amyloid, mouse, model, AD”. 38% (21/56) of these papers provided detailed information about use of different hemispheres for histology and biochemistry. 81% among those (17/21) assigned a specific hemisphere to a given modality, whereas only 19% (4/21) performed randomization of hemispheres to different modalities. Most of the remaining 35 papers likewise split hemispheres to different modalities, but without detailed information about the selection process. Immunohistochemistry with Aβ antibodies like 6E10 was most frequently used to assess fibrillar plaques *in vitro*, whereas other studies used histological staining with methoxy-X04 or thioflavin S (*14,25*). These studies generally reported immunohistochemistry/histology findings for Aβ quantification from a few representative brain slices of a single hemisphere, whereas the other hemisphere was typically reserved for biochemical assays such as Enzyme-linked Immunosorbent Assay or western blotting, which are not compatible with tissue fixation. Therefore, evaluation of intra-animal asymmetry *in vitro* was not feasible due to allocation of the hemispheres for different kinds of analyses. In

summary, potential asymmetries of fibrillar plaque burden were only sparsely considered in published papers during the recent years.

Contrary to the case *in vitro*, Aβ-PET allows convenient quantification of amyloid pathology in both whole hemispheres, with the caveat that the PET method has inherent limitations in spatial resolution (*26,27*). Therefore, PET quantification of small brain areas can be challenging, although asymmetry assessment Aβ plaque burden in large forebrain regions is a rather robust measure. Thus, conducting non-invasive PET examination prior to assignment of hemispheres to different terminal biochemical or histological experiments could help to identify and adjust for relevant asymmetries of plaque burden. This should encourage the combined use of PET together with immuno(histochemistry) and biochemistry read outs.

Another focus of our study was to investigate the relationship between lateralized Aβ deposition and microglial activation. Previous studies of our laboratory have already shown close correlations between fibrillar amyloidosis and TSPO expression in APP/PS1, PS2APP, APP-SL70 and $App^{NL\text{-}G\text{-}F}$ mice (*3,4,10,16*). Although we acknowledge that it was anticipated from these earlier findings, we now show for the first time that microglial activation occurs concomitantly in the hemisphere ipsilateral with predominant fibrillar amyloidosis. This association further strengthens the hypothesis that initial fibrillar Aβ accumulation triggers neuroinflammation mediated by activated microglia (*28*). Another recently published study has also demonstrated a link between amyloidosis and neuroinflammation based on comparative profiling of cortical gene expression in AD patients and an Aβ mouse model (*29*). Comparisons of gene expression between hemispheres of mice with asymmetric amyloidosis could give new insights into the molecular pathways and causal mechanisms underlying asymmetry in AD. PET screening could guide the selection for detailed study of mice with strong asymmetries.

## CONCLUSION

Nearly a third of Aβ mice show distinct left- or right-asymmetry in the deposition of cerebral amyloid. This phenomenon is neglected in the majority of current studies in Aβ mice and calls for consideration in the planning and design of preclinical trials, especially when single hemispheres are investigated by methods *ex vivo*. The lack of age-dependency on asymmetric Aβ distribution implies that genetic factors underlie the development of lateralized amyloidosis in AD model mice. There is a clear association between asymmetries of glial activation and fibrillar amyloidosis in all Aβ mouse models investigated in this study, further strengthening the hypothesis that neuroinflammatory response to fibrillar Aβ contribute to the development of pathology in these mice.

## DISCLOSURE

C.H. collaborates with Denali Therapeutics, participated on one advisory board meeting of Biogen, and received a speaker honorarium from Novartis and Roche. C.H. is chief advisor of ISAR Bioscience. P.B., A.R. and M.B. received speaking honoraria from Life Molecular Imaging and GE healthcare. M.B. is an advisor of Life Molecular Imaging. No other potential conflicts of interest relevant to this article exist.

## ACKNOWLEDGEMENTS

C.H. is supported by the Koselleck Project HA1737/16-1 of the DFG, the Helmholtz-Gemeinschaft (Zukunftsthema"Immunology and Inflammation"(ZT-0027)) and the Cure Alzheimer's fund. The work was supported by the Deutsche Forschungsgemeinschaft (M.B. and A.R. BR4580/1-1&RO5194/1-1). The APPPS1 colony was established from a breeding pair kindly provided by M. Jucker (Hertie-Institute for Clinical Brain Research, University of Tübingen and DZNE-Tübingen). APPswe, PS2APP and APP-SL70 mice were provided by Hoffmann-La Roche.

*APP*$^{NL-G-F}$ mice were provided by RIKEN BRC through the National Bio-Resource Project of the MEXT, Japan. GE Healthcare made GE-180 cassettes available through an early-access model.

QUESTION: Do amyloid mouse models have asymmetric plaque distribution and asymmetric neuroinflammation?

PERTINENT FINDINGS: Asymmetry in these amyloid mouse models is frequent and statistically relevant for planning of observational and interventional trials in these mice. Moreover, asymmetries of fibrillar plaque burden and glial activation are positively correlated.

TRANSLATIONAL IMPLICATIONS: Lateralized distribution of fibrillar plaques is insufficiently considered in experimental studies with amyloid mouse models and a potential confounder in preclinical phases of drug development.

## REFERENCES


**1.** Ziegler-Graham K, Brookmeyer R, Johnson E, Arrighi HM. Worldwide variation in the doubling time of Alzheimer's disease incidence rates. *Alzheimers Dement.* 2008;4:316-323.

**2.** Heneka MT, Carson MJ, El Khoury J, et al. Neuroinflammation in Alzheimer's disease. *Lancet Neurol.* 2015;14:388-405.

**3.** Sacher C, Blume T, Beyer L, et al. Longitudinal PET Monitoring of Amyloidosis and Microglial Activation in a Second-Generation Amyloid-beta Mouse Model. *J Nucl Med.* 2019;60:1787-1793.

**4.** Brendel M, Probst F, Jaworska A, et al. Glial Activation and Glucose Metabolism in a Transgenic Amyloid Mouse Model: A Triple-Tracer PET Study. *J Nucl Med.* 2016;57:954-960.

**5.** Sasaguri H, Nilsson P, Hashimoto S, et al. APP mouse models for Alzheimer's disease preclinical studies. *The EMBO Journal.* 2017;36:2473-2487.

**6.** Ossenkoppele R, Schonhaut DR, Scholl M, et al. Tau PET patterns mirror clinical and neuroanatomical variability in Alzheimer's disease. *Brain.* 2016;139:1551-1567.

**7.** Tetzloff KA, Graff-Radford J, Martin PR, et al. Regional Distribution, Asymmetry, and Clinical Correlates of Tau Uptake on [18F]AV-1451 PET in Atypical Alzheimer's Disease. *J Alzheimers Dis.* 2018;62:1713-1724.

**8.** Frings L, Hellwig S, Spehl TS, et al. Asymmetries of amyloid-beta burden and neuronal dysfunction are positively correlated in Alzheimer's disease. *Brain.* 2015;138:3089-3099.

**9.** Radde R, Bolmont T, Kaeser SA, et al. Abeta42-driven cerebral amyloidosis in transgenic mice reveals early and robust pathology. *EMBO Rep.* 2006;7:940-946.

**10.** Parhizkar S, Arzberger T, Brendel M, et al. Loss of TREM2 function increases amyloid seeding but reduces plaque-associated ApoE. *Nat Neurosci.* 2019;22:191-204.

**11.** Richards JG, Higgins GA, Ouagazzal AM, et al. PS2APP transgenic mice, coexpressing hPS2mut and hAPPswe, show age-related cognitive deficits associated with discrete brain amyloid deposition and inflammation. *J Neurosci.* 2003;23:8989-9003.

**12.** Ozmen L, Albientz A, Czech C, Jacobsen H. Expression of transgenic APP mRNA is the key determinant for beta-amyloid deposition in PS2APP transgenic mice. *Neurodegener Dis.* 2009;6:29-36.

**13.** Brendel M, Jaworska A, Overhoff F, et al. Efficacy of chronic BACE1 inhibition in PS2APP mice depends on the regional Abeta deposition rate and plaque burden at treatment initiation. *Theranostics.* 2018;8:4957-4968.

**14.** Brendel M, Kleinberger G, Probst F, et al. Increase of TREM2 during Aging of an Alzheimer's Disease Mouse Model Is Paralleled by Microglial Activation and Amyloidosis. *Front Aging Neurosci.* 2017;9:8.

**15.** Blanchard V, Moussaoui S, Czech C, et al. Time sequence of maturation of dystrophic neurites associated with Abeta deposits in APP/PS1 transgenic mice. *Exp Neurol.* 2003;184:247-263.

**16.** Blume T, Focke C, Peters F, et al. Microglial response to increasing amyloid load saturates with aging: a longitudinal dual tracer in vivo muPET-study. *J Neuroinflammation.* 2018;15:307.

**17.** Masuda A, Kobayashi Y, Kogo N, Saito T, Saido TC, Itohara S. Cognitive deficits in single App knock-in mouse models. *Neurobiol Learn Mem.* 2016;135:73-82.

**18.** Saito T, Matsuba Y, Mihira N, et al. Single App knock-in mouse models of Alzheimer's disease. *Nat Neurosci.* 2014;17:661-663.

**19.** Rominger A, Brendel M, Burgold S, et al. Longitudinal assessment of cerebral beta-amyloid deposition in mice overexpressing Swedish mutant beta-amyloid precursor protein using 18F-florbetaben PET. *J Nucl Med.* 2013;54:1127-1134.

**20.** Brendel M, Jaworska A, Herms J, et al. Amyloid-PET predicts inhibition of de novo plaque formation upon chronic gamma-secretase modulator treatment. *Mol Psychiatry.* 2015;20:1179-1187.

**21.** Overhoff F, Brendel M, Jaworska A, et al. Automated Spatial Brain Normalization and Hindbrain White Matter Reference Tissue Give Improved [(18)F]-Florbetaben PET Quantitation in Alzheimer's Model Mice. *Front Neurosci.* 2016;10:45.

**22.** Raji CA, Becker JT, Tsopelas ND, et al. Characterizing regional correlation, laterality and symmetry of amyloid deposition in mild cognitive impairment and Alzheimer's disease with Pittsburgh Compound B. *J Neurosci Methods.* 2008;172:277-282.

**23.** Manook A, Yousefi BH, Willuweit A, et al. Small-animal PET imaging of amyloid-beta plaques with [11C]PiB and its multi-modal validation in an APP/PS1 mouse model of Alzheimer's disease. *PLoS One.* 2012;7:e31310.

**24.** Brendel M, Jaworska A, Griessinger E, et al. Cross-sectional comparison of small animal [18F]-florbetaben amyloid-PET between transgenic AD mouse models. *PLoS One.* 2015;10:e0116678.

**25.** Cho SM, Lee S, Yang SH, et al. Age-dependent inverse correlations in CSF and plasma amyloid-beta(1-42) concentrations prior to amyloid plaque deposition in the brain of 3xTg-AD mice. *Sci Rep.* 2016;6:20185.

**26.** Visser EP, Disselhorst JA, Brom M, et al. Spatial resolution and sensitivity of the Inveon small-animal PET scanner. *J Nucl Med.* 2009;50:139-147.

**27.** Huisman MC, Reder S, Weber AW, Ziegler SI, Schwaiger M. Performance evaluation of the Philips MOSAIC small animal PET scanner. *Eur J Nucl Med Mol Imaging.* 2007;34:532-540.

**28.** Monasor LS, Müller SA, Colombo A, et al. Fibrillar Aβ triggers microglial proteome alterations and dysfunction in Alzheimer mouse models. *bioRxiv.* 2019:861146.

**29.** Castillo E, Leon J, Mazzei G, et al. Comparative profiling of cortical gene expression in Alzheimer's disease patients and mouse models demonstrates a link between amyloidosis and neuroinflammation. *Sci Rep.* 2017;7:17762.

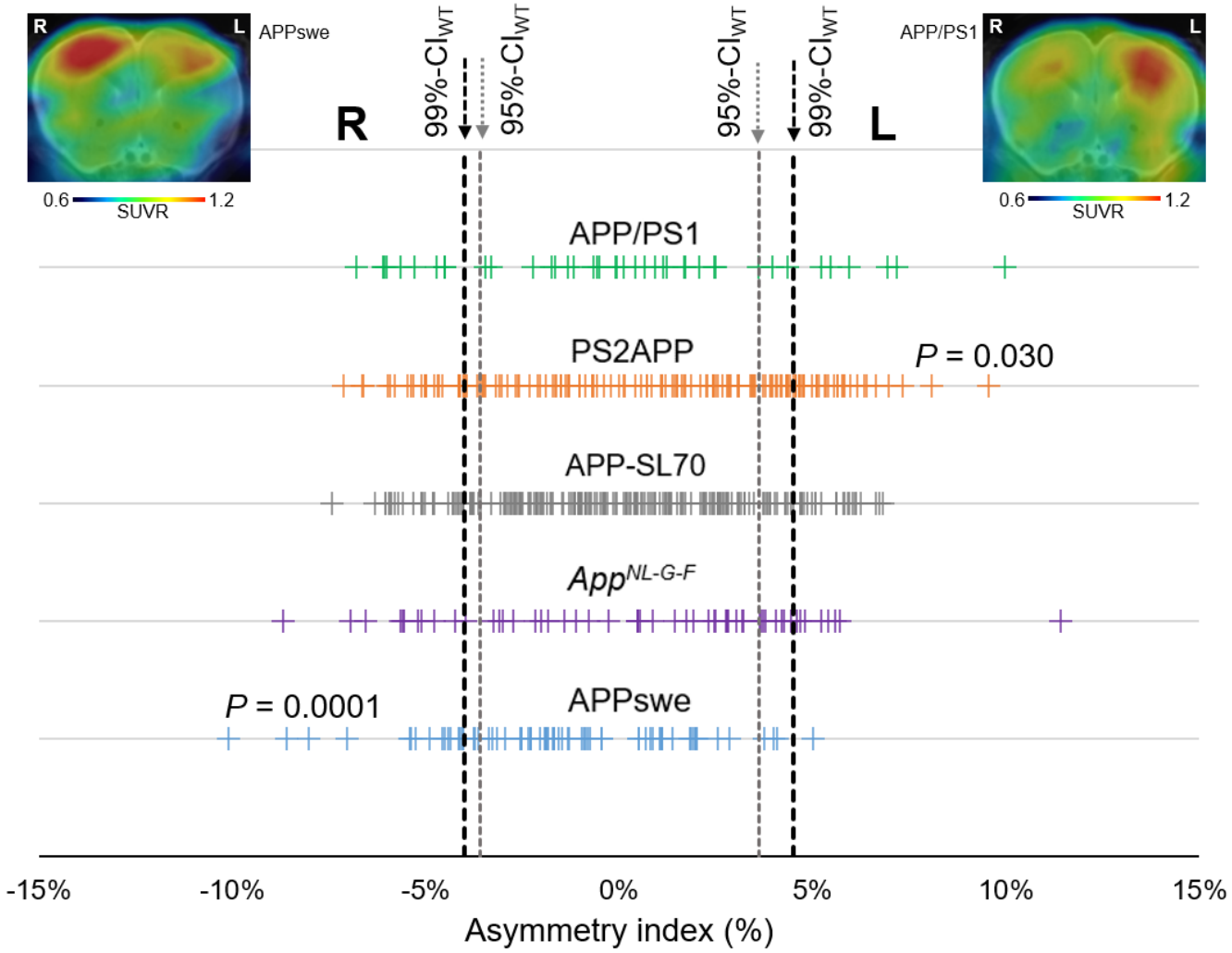


**Figure 1 – Asymmetry of plaque distribution in amyloid mouse models.** Forrest plot shows AI for a total of 523 amyloid PET scans in APP/PS1, PS2APP, APP-SL70, APPswe and *App*$^{NL-G-F}$ mice. Lateralized plaque distributions were compared by a Chi-square test to test for left or right predominance in each mouse model. Representative PET SUVR-images show exemplary mice with right (APPSwe) and left (APP/PS1) asymmetry.

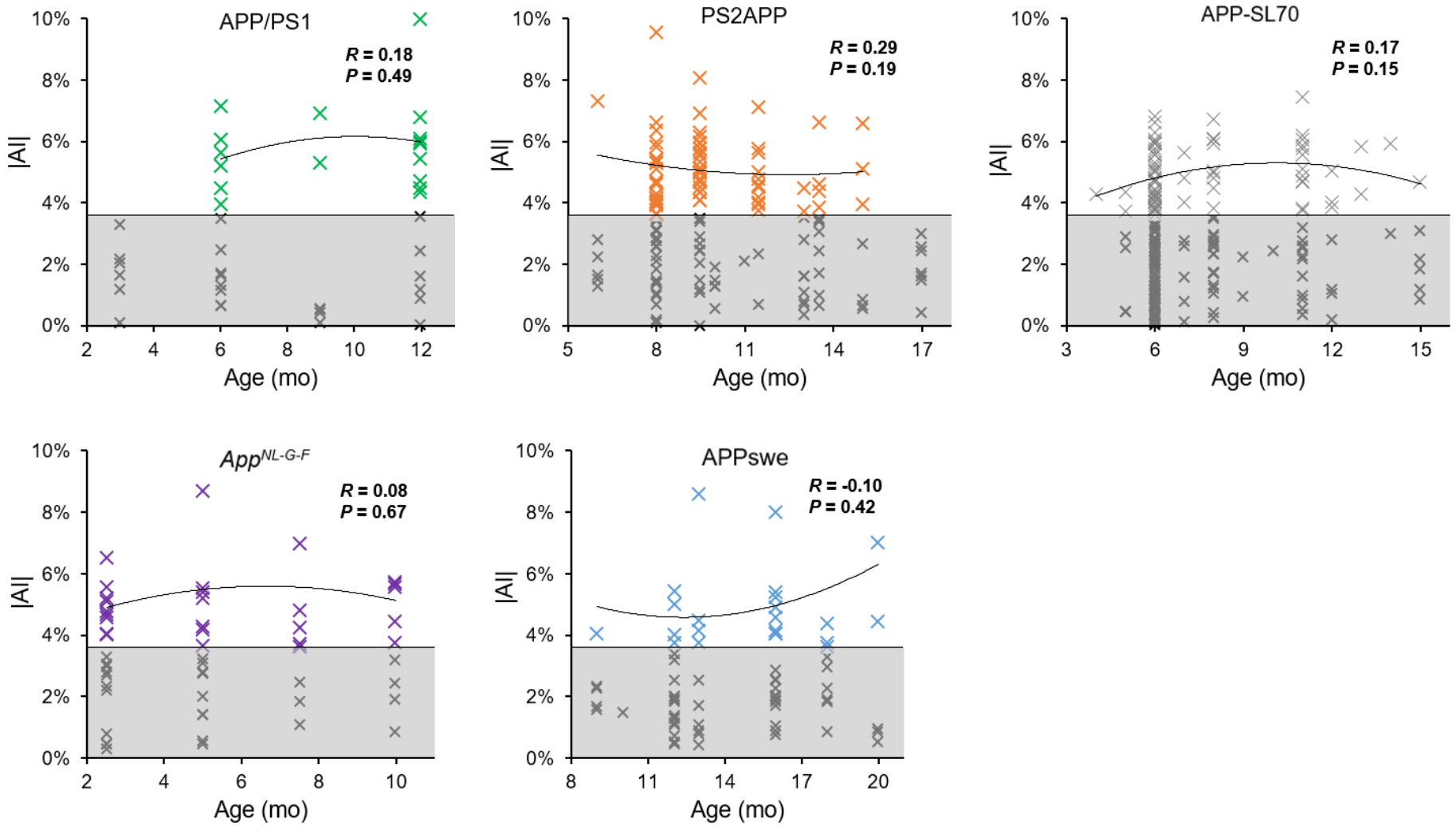


**Figure 2 – Age dependency of asymmetric amyloid deposition.** Asymmetry (|AI|) is shown as a function of age for APP/PS1, PS2APP, APP-SL70, APPswe and *App*$^{NL\text{-}G\text{-}F}$ mice. Datapoints with significant asymmetric $^{18}$F-FBB uptake (|AI| > 95%-CI$_{WT}$; light area) indicate no relevant dependency on asymmetric plaque distribution on age in any of the mouse models. Values with symmetric distribution (grey area) were excluded from the correlation analysis.

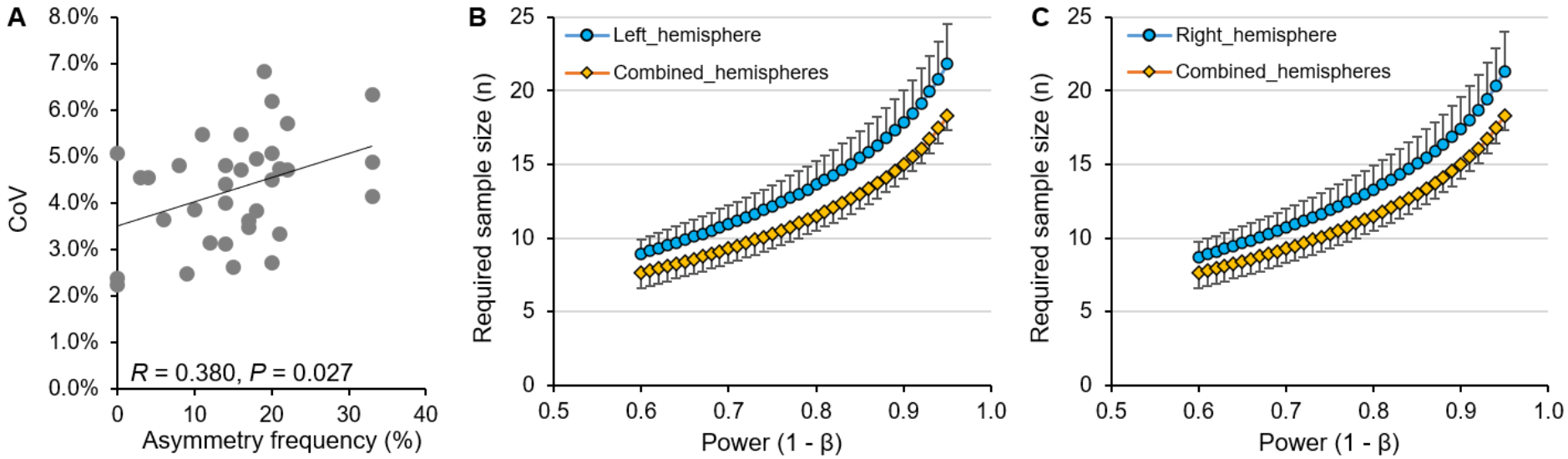


**Figure 3 – Statistical relevance of asymmetric plaque distribution in amyloid mouse models.** (**A**) Association of higher coefficients of variation (CoV) in SUVR with higher frequency of asymmetry in age related groups of amyloid mouse models (see supplemental Table 1). (**B, C**) Required sample sizes as a function of power in comparison of analyses in single hemispheres and combined hemispheres (given effect of 5%, α=0.05, hypothetical 2-sided t-test of independent measures).

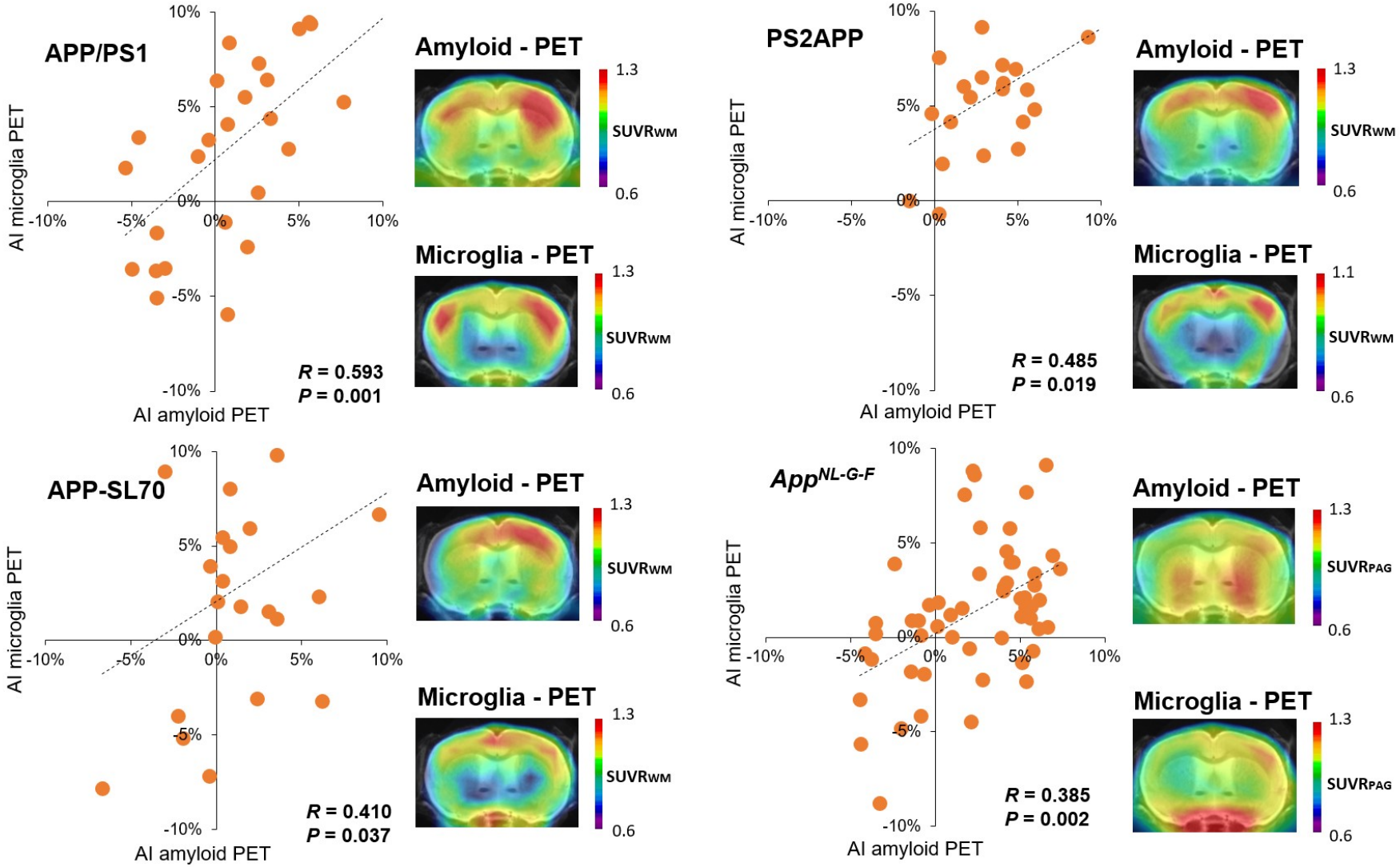


**Figure 4 - Association between lateralized amyloid deposition and microglia activation.** Correlations between AIs of amyloid and microglia PET in APP/PS1, PS2APP, APP-SL70 and *App*$^{NL-G-F}$ mice show congruent asymmetry of both biomarkers. *R* indicates Pearson's coefficients of correlation.

| Group | Age (months) | Amyloid-PET | | | | | | | | | TSPO-PET |
|---|---|---|---|---|---|---|---|---|---|---|---|
| | | n | Moderate asymmetry (>/< 95%-CI$_{WT}$) | | | | Strong asymmetry (>/< 99%-CI$_{WT}$) | | | | n |
| | | | Left (n, % per subgroup) | Left (n, % per model) | Right (n, % per subgroup) | Right (n, % per model) | Left (n, % per subgroup) | Left (n, % per model) | Right (n, % per subgroup) | Right (n, % per model) | |
| **APP/PS1** | 3 | 6 | 0 ( 0%) | 20% | 0 ( 0%) | 22% | 0 ( 0%) | 15% | 0 ( 0%) | 22% | 0 |
| | 6 | 14 | 3 (21%) | | 3 (21%) | | 2 (14%) | | 3 (21%) | | 14 |
| | 9 | 6 | 1 (16%) | | 1 (17%) | | 1 (17%) | | 1 (17%) | | 5 |
| | 12 | 15 | 4 (27%) | | 5 (33%) | | 3 (20%) | | 5 (33%) | | 8 |
| **PS2APP** | 6 - 8 | 55 | 15 (27%) | 30% | 12 (22%) | 19% | 10 (18%) | 21% | 9 (16%) | 16% | 13 |
| | 9 - 10 | 42 | 16 (38%) | | 9 (21%) | | 14 (33%) | | 9 (21%) | | 10 |
| | 11 - 14 | 36 | 12 (33%) | | 5 (14%) | | 7 (19%) | | 4 (11%) | | 0 |
| | 15 - 17 | 14 | 1 ( 7%) | | 2 (20%) | | 0 ( 0%) | | 2 (14%) | | 0 |
| **APP-SL70** | 4 - 6 | 130 | 21 (16%) | 18% | 20 (15%) | 16% | 12 ( 9%) | 12% | 16 (12%) | 13% | 0 |
| | 7 - 9 | 37 | 6 (16%) | | 6 (16%) | | 5 (14%) | | 5 (14%) | | 8 |
| | 10 - 12 | 31 | 8 (26%) | | 7 (23%) | | 6 (19%) | | 5 (16%) | | 10 |
| | 13 - 15 | 10 | 3 (30%) | | 1 (10%) | | 2 (20%) | | 1 (10%) | | 8 |
| ***App$^{NL-G-F}$*** | 2.5 | 20 | 4 (20%) | 29% | 5 (25%) | 20% | 3 (15%) | 10% | 4 (20%) | 18% | 17 |
| | 5 | 17 | 4 (24%) | | 3 (18%) | | 1 ( 6%) | | 3 (18%) | | 15 |
| | 7.5 | 9 | 4 (44%) | | 2 (22%) | | 2 (22%) | | 2 (22%) | | 11 |
| | 10 | 9 | 4 (44%) | | 1 (11%) | | 2 (22%) | | 1 (11%) | | 12 |
| **APPswe** | 9 - 12 | 26 | 3 (12%) | 6% | 2 ( 8%) | 26% | 1 ( 4%) | 2% | 2 ( 8%) | 22% | 0 |
| | 13 - 16 | 30 | 1 ( 3%) | | 11 (37%) | | 0 ( 3%) | | 10 (33%) | | 0 |
| | 17 - 20 | 16 | 0 ( 0%) | | 6 (38%) | | 0 ( 0%) | | 4 (25%) | | 0 |
| | | | | | | | | | | | |
| **C57BL/6 (wild-type)** | 2.5 - 16 | 27 | | | | | | | | | |

**Supplemental Table 1 – Overview of the animal cohorts studied by Aβ-PET and TSPO-PET and their frequency of asymmetry in Aβ-PET**